Solid-State Electronics 52 (2008) 1829–1832

Contents lists available at ScienceDirect

Solid-State Electronics

journal homepage: www.elsevier.com/locate/sse

InAs-based heterostructure barrier varactor diodes with $In_{0.3}Al_{0.7}As_{0.4}Sb_{0.6}$ as the barrier material

James G. Champlain *, Richard Magno, Mario Ancona, Harvey S. Newman, J. Brad Boos

Naval Research Laboratory, 4555 Overlook Avenue SW, Washington, DC 20375, United States

ARTICLE INFO

Article history:
Received 30 June 2008
Received in revised form 11 August 2008
Accepted 13 August 2008

Keywords:
Heterobarrier varactor
Sb-base semiconductors

ABSTRACT

InAs-based heterostructure barrier varactor (HBV) diodes with $In_{0.3}Al_{0.7}As_{0.4}Sb_{0.6}$ as the barrier material are demonstrated. Current–voltage and capacitance–voltage characteristics, as well as *S*-parameters, of HBV diodes with varying barrier thicknesses are examined. Maximum capacitance values and maximum-to-minimum capacitance ratios greater than those predicted by traditional HBV models were measured. The HBVs' unconventional behavior in terms of charge accumulation layers adjacent to the wide bandgap barrier is discussed.

Published by Elsevier Ltd.

1. Introduction

Heterostructure barrier varactor (HBV) diodes are desirable devices for use in high-frequency multiplier circuits. The HBV is a symmetric varactor and therefore, in a multiplier circuit, generates only odd harmonics and requires no DC bias for operation. As compared to a multiplier circuit employing conventional Schottky varactors, this reduces the required number of idlers and, thereby, the complexity of the circuit design, in addition to reducing the DC power consumption of the circuit. Furthermore, multiple barriers may be added to the varactor layer structure, increasing its power handling capabilities without increasing its footprint [1–3].

Previous HBV diodes in the $Al_xGa_{1-x}As$/GaAs material system suffered from poor efficiencies as a result of high leakage currents, a consequence of the low conduction band offset between GaAs and AlAs ($\Delta E_{C,GaAs/AlAs} = 0.27$ eV) [4,5]. Diodes in the InP lattice-matched material system, using strained AlAs as the barrier material, have shown improved performances (*e.g.*, increased power output, increased efficiencies) over their $Al_xGa_{1-x}As$/GaAs counterparts due to the increased conduction band offset (~1.0 eV) and conductivity of $In_{0.53}Ga_{0.47}As$. But, due to the difficulties associated with growing strained AlAs on InP, the design and fabrication of these devices becomes more complicated [5–7].

By adapting the HBV diode to Sb-based material systems, improvements in performance could be seen over those in the $Al_xGa_{1-x}As$/GaAs and InP lattice-matched systems due to: the increased conduction band offset between InAs and the various Sb-based, wide bandgap semiconductors (AlSb: $\Delta E_C \approx 1.4$ eV, $In_{0.3}Al_{0.7}As_{0.4}Sb_{0.6}$: $\Delta E_C \approx 1.1$ eV) [8], which will lead to reduced leakage currents; the lack of any restriction on barrier thickness due to a lattice-matched wide bandgap material, which will allow greater flexibility in device design; a narrow bandgap material for low contact resistance; and a high mobility/high saturation velocity material for low series resistances and, therefore, high-frequency response.

In this paper, we demonstrate the first InAs-based HBV diodes fabricated with $In_{0.3}Al_{0.7}As_{0.4}Sb_{0.6}$ as the wide bandgap barrier material. $In_{0.3}Al_{0.7}As_{0.4}Sb_{0.6}$ is chosen as the wide bandgap barrier material because it offers a valence band barrier ($\Delta E_V \approx$ 100 meV) in addition to a conduction band barrier and being lattice-matched, whereas no valence band barrier exists between InAs and AlSb, as seen from the InAs (Fig. 1). Current–voltage and capacitance–voltage characteristics, as well as *S*-parameters, of diodes with varying barrier thicknesses are examined. Their behavior in terms of traditional HBVs and HBV models is discussed.

2. Device growth and fabrication

HBV diode samples were grown by solid-source molecular beam epitaxy (MBE). The layer structure consisted of, from

* Corresponding author. Tel.: +1 202 404 4620; fax: +1 202 767 0455.
E-mail address: james.champlain@nrl.navy.mil (J.G. Champlain).

0038-1101/$ - see front matter Published by Elsevier Ltd.
doi:10.1016/j.sse.2008.08.005

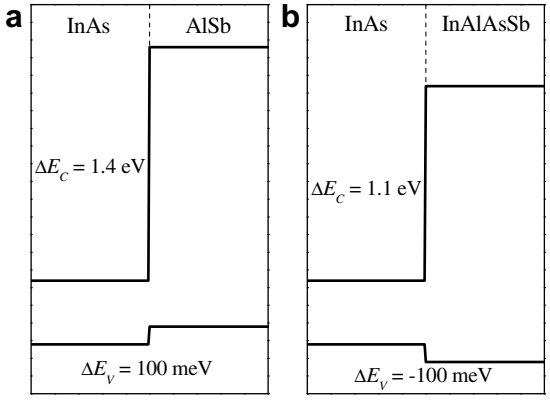

Fig. 1. Conduction and valence band line-up for (a) InAs and AlSb and (b) InAs and $In_{0.3}Al_{0.7}As_{0.4}Sb_{0.6}$ (labeled InAlAsSb in the diagram).

substrate to surface, a semi-insulating (SI) InP substrate, a 2000 Å undoped, lattice-matched $In_{0.52}Al_{0.48}As$ buffer, a 1000 Å undoped InAs buffer, a 7650 Å n (Te: 1×10^{17} cm^{-3}) InAs contact/modulation layer, a 50 Å undoped InAs spacer layer, the wide bandgap $In_{0.3}Al_{0.7}As_{0.4}Sb_{0.6}$ barrier layer, another 50 Å undoped InAs spacer layer, a 1500 Å n (Te: 1×10^{17} cm^{-3}) InAs modulation layer, and a 100 Å n^+ (Te: 1×10^{18} cm^{-3}) InAs contact layer. The $In_{0.3}Al_{0.7}As_{0.4}Sb_{0.6}$ layer was grown as a short-period superlattice consisting of repeated layers of 2 ML of $In_{0.3}Al_{0.7}As$ and 3 ML of $In_{0.3}Al_{0.7}Sb$. The superlattice was terminated with 2 ML of $In_{0.3}Al_{0.7}As$ in order to provide a symmetric barrier with identical interfaces to the two InAs modulation layers (Fig. 2). Three structures with the following barrier thicknesses were grown: 100 Å, 200 Å, and 300 Å. Fig. 3 shows the out-of-plane X-ray diffraction scan for the structure with the 200 Å thick barrier. The measured lattice constant for the InAs and barrier layers was approximately 6.059 Å for all samples with full-width at half-maximums (FWHMs) of 392″, 427″, and 408″ for the 100 Å, 200 Å, and 300 Å barrier structures, respectively.

The HBV diodes were fabricated in a mesa diode configuration using standard processing techniques. Diode mesas were first defined using optical lithography and a H_3PO_4:H_2O_2:H_2O (1:1:10) etch mixture. The diodes were etched to a depth approximately 1550 Å below the wide bandgap barrier, mimicking the thickness of the top modulation and spacer layers. Top and bottom contacts were defined simultaneously using optical lithography, and Ti:Pt:Au (100:50:2500 Å) unannealed, Ohmic contacts were deposited by e-beam evaporation. The diode mesa to bottom (cathode)

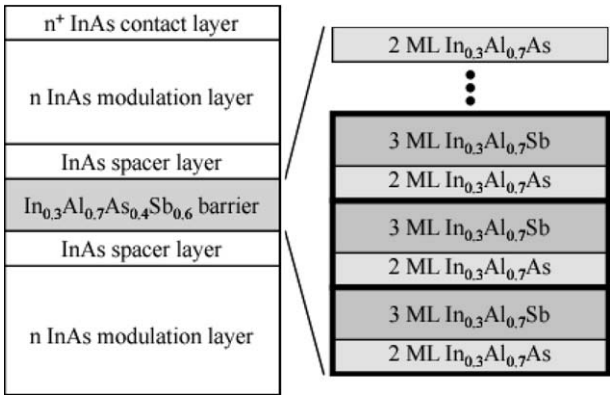

Fig. 2. Layer structure of the InAs-based HBV with $In_{0.3}Al_{0.7}As_{0.4}Sb_{0.6}$ as the wide bandgap barrier. The $In_{0.3}Al_{0.7}As_{0.4}Sb_{0.6}$ is grown as a short-period superlattice of 2 ML $In_{0.3}Al_{0.7}As$ and 3 ML $In_{0.3}Al_{0.7}Sb$ with a final 2 ML $In_{0.3}Al_{0.7}As$ layer.

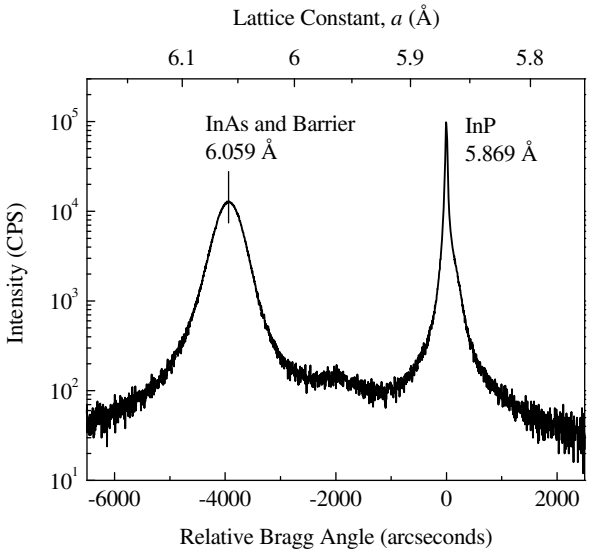

Fig. 3. Out-of-plane X-ray diffraction scan for the HBV diode structure with the 200 Å thick barrier. The InAs and $In_{0.3}Al_{0.7}As_{0.4}Sb_{0.6}$ lattice constant is 6.095 Å with a full-width at half-maximum of 427″.

contact spacing was 4 μm. Prior to contact evaporation, an oxygen-plasma descum and oxide removal dip in HCl:H_2O (1:10) was performed.

3. Measurement, results, and discussion

The DC current–voltage characteristics for the three structures are shown in Fig. 4. It can be clearly seen that as the barrier thickness is reduced the current level increases. The dependence of the current level on barrier thickness suggests that current transport in these devices is, at least, dominated by tunneling through the wide bandgap barrier, if not solely due to it, as opposed to thermionic emission over the barrier, which would essentially be barrier thickness independent.

Fig. 5 shows the capacitance–voltage (CV) characteristics for the three structures taken at 10 MHz using a LCR meter. The LCR meter assumes a simple parallel resistor–capacitor (RC) model in its determination of capacitance. The devices show near −90° phase around zero bias, demonstrating the highly capacitive nature of these devices. The phase rapidly climbs to 0° at higher biases,

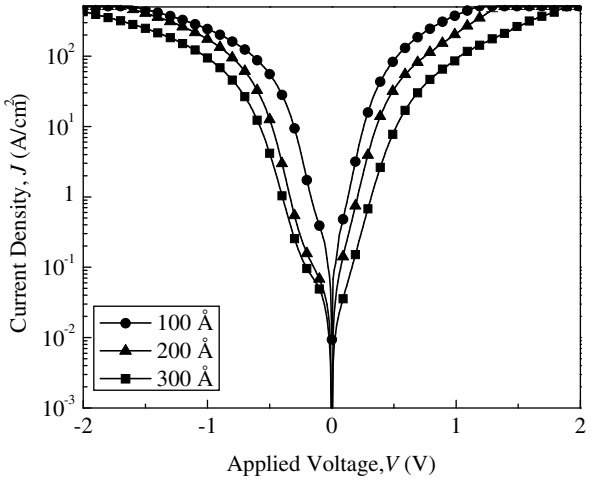

Fig. 4. Plot of current density (J) versus applied voltage (V) for the three HBV diode structures.

which is a result of the increase in conduction current through the device and associated increase in conductance with bias. Due to the simplistic nature of the assumed parallel *RC* model used, the *CV* measurements become inaccurate as the phase moves away from −90°. For more accurate measurements of the *CV* characteristics for the three structures, *S*-parameter measurements were performed.

By applying a more accurate and correct model of the HBV to the measured *S*-parameter data, a more accurate *CV* characteristic can be extracted over a broader range of bias. The improved model consisted of a parallel combination of resistance and capacitance, representing the intrinsic characteristics of the barrier, with an extrinsic series resistance, which accounts for the sum total of the resistances outside of the intrinsic device (*e.g.*, the bulk series resistance leading up to the barrier and depletion regions and the top and bottom contact resistances). Fig. 6 shows an example of the improved model applied to measured *S*-parameter data. For comparison, a simple *RC* parallel pair is also plotted.

Fig. 7 shows the *CV* characteristics as extracted from *S*-parameters for all three structures. For comparison, plots of *CV* characteristics using the Chalmers HBV diode model applied to the 100 Å and 300 Å structures are included. The Chalmers HBV diode model determines the capacitance of the HBV using a novel charge–voltage relationship that is empirically derived using a classical depletion layer analysis and includes screening effects for low biases, where the classical analysis commonly fails to predict the capacitance properly [2]. From the figure, at low biases, the measured capacitance is large relative to the Chalmers model. As the bias is increased, the measured capacitance approaches that of the Chalmers model. This suggests that some other phenomenon, outside of what is modeled in the Chalmers model, is occurring at lower biases. At higher biases, this phenomenon diminishes or is removed and the HBV returns to the classical depletion behavior described by the Chalmers model.

In order to achieve capacitances larger than those predicted by the Chalmers model, the depletion width at the relative bias must be smaller. To achieve a smaller depletion width at or near zero bias, relative to that dictated by simple depletion, requires the presence of charge accumulation layers near the barrier, which would result in a dramatic drop in the depletion width and an associated increase in capacitance. As these accumulation layers are depleted, the depletion width moves outward and away from the barrier until the accumulation layer is fully depleted and the HBV returns to the depletion physics employed by the Chalmers model, resulting in a behavior predicted by the model. This behavior is identical to the reverse bias behavior of a doped-channel high-electron mobility transistor (HEMT). Device physics simulations of the 200 Å HBV (using ATLAS from Silvaco International), incorporating charge accumulation layers next to the barrier, agree well with the measured results, supporting this hypothesis (Fig. 8).

The exact source of these accumulation layers is as of yet unknown, but is believed to be due to diffused tellurium (Te) dopant from the lower modulation layer into the wide bandgap barrier resulting in a modulation doping effect. The simulations performed for this paper employed fixed charge within the barrier as the source for the accumulated charge. These simulations and the device model, which agrees well with the measured data up to the maximum measured frequency of 50 GHz, suggest that any charge

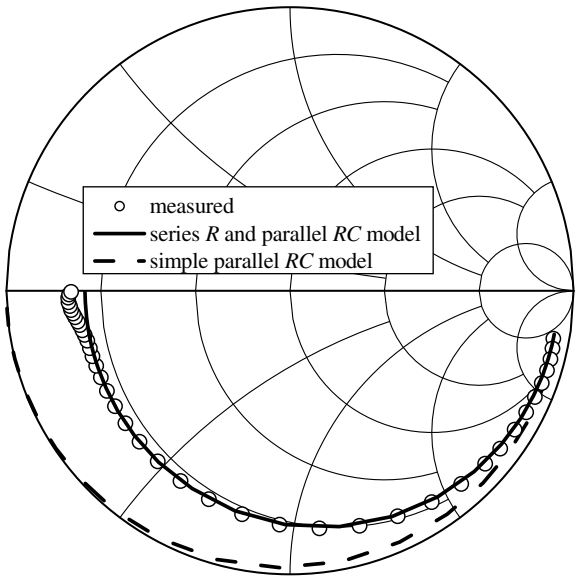

Fig. 6. Plot of the *S*-parameter characteristics of the improved HBV lumped element model versus measured *S*-parameter data. The measured *S*-parameter data is of the 200 Å barrier HBV diode measured at an applied bias of −0.1 V from 10 MHz to 50 GHz. The model consists of an 8.05 Ω resistor in series with a parallel 1789 Ω resistor and 26.2 pF capacitor, plotted over the same frequency range. For comparison, the *S*-parameter characteristics of a simple parallel resistor–capacitor pair (R = 1759 Ω, C = 26.2 pF) is shown.

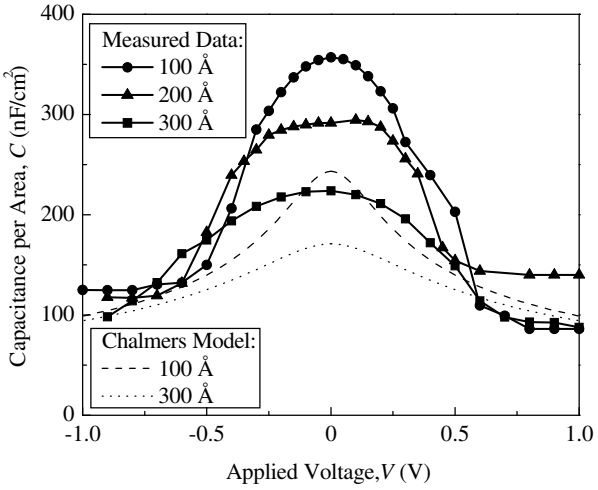

Fig. 7. Plot of capacitance per unit area extracted from *S*-parameters (C) versus applied voltage (V) for the three HBV diode structures. The upper dashed curve is the *CV* characteristic for a 100 Å barrier HBV using the Chalmers model. The lower dotted curve is the *CV* characteristic for a 300 Å barrier HBV using the Chalmers model.

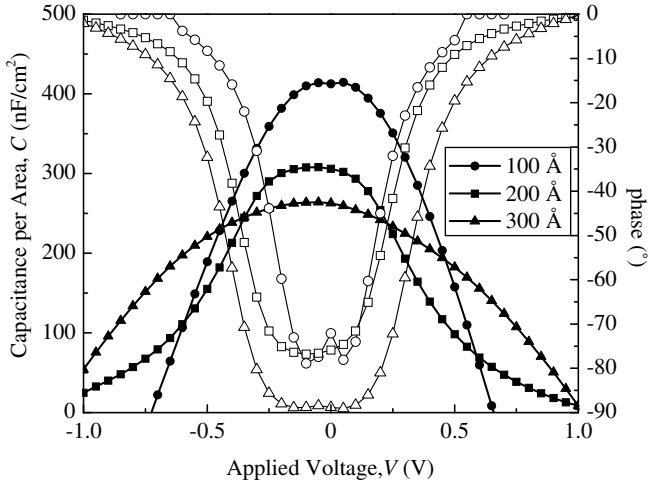

Fig. 5. Plot of capacitance per unit area (C) versus applied voltage (V) for the HBV diode samples measured using an LCR meter.

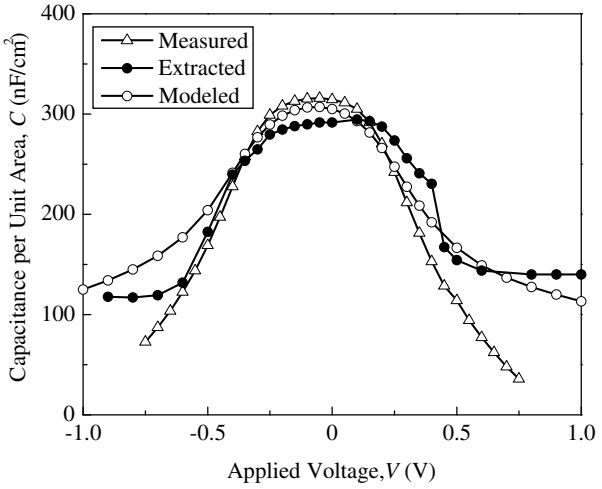

Fig. 8. Plot of capacitance per unit area (*C*) versus applied voltage (*V*) for the 200 Å barrier HBV structure measured using an LCR meter (Measured, open triangles), extracted from *S*-parameters (Extracted, solid circles), and simulated (Modeled, open circles).

that is present within the barrier, either fixed or ionized Te, has little or no impact on the frequency performance of the HBV over the measured range.

4. Conclusion

InAs-based HBVs using $In_{0.3}Al_{0.7}As_{0.4}Sb_{0.6}$ as the barrier material have been demonstrated for the first time. Current–voltage and capacitance–voltage characteristics have been measured for three barrier thickness: 100, 200, and 300 Å. Current–voltage measurements showed that the current within these HBVs was dependent upon the barrier thickness, suggesting tunneling through the wide bandgap barrier is the dominant current transport mechanism. The exact nature of current transport in these HBVs has not yet been determined. *S*-parameter measurements were made; and a model for the HBV consisting of a parallel resistance and capacitance, representing the intrinsic barrier, and a series extrinsic resistance was developed. Symmetric *CV* profiles, characteristic of HBVs, have been measured, but capacitances higher than those anticipated by the Chalmers model and simple depletion physics have been observed. It has been hypothesized that the source of the higher than expected capacitance is charge accumulation layers adjacent to the barrier. Device physics modeling supports this hypothesis. Future work on the exact nature of current transport through the HBV and the *CV* behavior of the HBV is planned.

References

[1] Jones JR, Bishop WL, Jones SH, Tait GB. Planar multibarrier 80/240-GHz heterostructure barrier varactor triplers. IEEE Trans Microwave Theory Tech 1997;45:512–8.
[2] Dillner L, Stake J, Kollberg EL. Modeling of the heterostructure barrier varactor diode. In: International semiconductor device research symposium (ISDRS), 1997.
[3] Ingvarson M, Olsen AØ, Stake J. Design and analysis of 500 GHz heterostructure barrier varactor quintuplers. In: Proceedings of the 14th international symposium on space terahertz technology, 2003.
[4] Fu Y, Stake J, Dillner L, Willander M, Kollberg EL. AlGaAs/GaAs and InAlAs/InGaAs heterostructure barrier varactors. J Appl Phys 1997;82:5568–72.
[5] Mélique X, Mann C, Mounaix P, Thornton J, Vanbésien O, Mollot F, et al. 5-mW and 5% efficiency 216-GHz InP-based heterostructure barrier varactor tripler. IEEE Microwave Guided Wave Lett 1998;8:384–6.
[6] Lheurette E, Mélique X, Mounaix P, Mollot F, Vanbésien O, Lippens D. Capacitance engineering for InP-based heterostructure barrier varactor. IEEE Electron Dev Lett 1998;19:338–40.
[7] Mélique X, Maestrini A, Farré R, Mounaix P, Favreau M, Vanbésien O, et al. Fabrication and performance of InP-based heterostructure barrier varactors in a 250 GHz waveguide tripler. IEEE Trans Microwave Theory Tech 2000;48:1000–6.
[8] Vurgaftman I, Meyer JR, Ram-Mohan LR. Band parameters for III–V compound semiconductors and their alloys. J Appl Phys 2001;89:5815–75.